Δ excitation and coherent pion production in charge exchange reactions

Swapan Das
Nuclear Physics Division, Bhabha Atomic Research Centre, Mumbai-400 085, India
(Received 17 October 2001; published 9 July 2002)

For the forward going ejectile, the Δ excitation and the coherent pion emission in the charge exchange reaction have been described by the real pion induced reaction. Using a pseudovector pion coupling to nucleon and the eikonally distorted waves for projectile and ejectile, the double differential cross section for the ejectile energy/momentum distribution is written in terms of the cross section for pion scattering on the nucleus. This cross section has been approximated by the corresponding measured cross section for the real pion. Calculated spectral shapes for various reactions agree very well with the measured distributions.

DOI: 10.1103/PhysRevC.66.014604 PACS number(s): 25.40.Kv, 13.75.−n

I. INTRODUCTION

Pion has a very special role as a cloud surrounding the nucleon, for example, for a part of the time a proton can be thought to be $p \rightarrow n + \pi^+$. Similarly, ^{3}He surrounds itself by a pion cloud through the virtual process $^3\mathrm{He} \rightarrow t + \pi^+$ [1]. This pion cloud can be visualized better by studying the quark aspect of a nucleon. To conserve the chiral symmetry for quark inside the nucleon, it is essential for pion to be at the surface of the nucleon. This makes a physical nucleon as a quark-gluon object surrounded by the pion itself. This pion cloud, as emphasized by Ericson and Weise [1], rides along with the incident beam, and can materialize as a controllable virtual pion beam in certain reactions those involve pionlike excitations. The four momentum carried by the virtual pion beam would be the same as that transferred from the projectile-ejectile vertex to nucleus. The charge exchange reactions, like (p,n) and $(^3\mathrm{He},t)$, are such class of reactions, where, at intermediate energies and for forward going ejectile, the cross section is found to be dominated by the pionlike spin-isospin Gamow-Teller excitations. Therefore, the data on these reactions provide an opportunity to explore the nuclear response to virtual pion, and also to investigate the difference of this response from that of a real pion.

Extensive measurements on the charge exchange reactions, covering nuclear excitations from low to intermediate energies, had been done at various accelerator facilities. Data exist on inclusive as well as on exclusive measurements. In the inclusive experiments at intermediate energies, the double differential cross sections for the ejectile energy/momentum distribution in the charge exchange reactions, such as n in (p,n) [2,3] and t in $(^3\mathrm{He},t)$ [4,5] reactions, were measured without detecting any other particles produced in the final state. All of these measured distributions distinctively show a bump at around 300 MeV nuclear excitation. Since this excitation energy lies in the vicinity of $\Delta(1232)$ excitation of a nucleon, this bump is understandably interpreted as the spin-isospin excitation of a nucleon in the nucleus to a Δ isobar. In the recent past, the most widely publicized issue in the inclusive measurements on $(^3\mathrm{He},t)$ reaction in this Δ excitation region was the downward shift of Δ-peak position by ~ 70 MeV in nuclear targets as compared to proton target [5]. This phenomenon, however, is also found to persist in the other charge exchange reactions such as (p,n) reaction [2]. In contrast to pion induced reactions, the position of Δ peak in the charge exchange reactions does not show much dependence on the target mass number.

The observation in the above inclusive measurements had generated a great deal of interest in the dynamics for the shift of Δ peak. Consequently, various models describing various origins for this shift were proposed by several authors [6]. In order to understand the origin for this peak shift and to disentangle the contributions from different channels to the inclusive spectra, the exclusive experiments had been done on (p,n) reaction at KEK [7] and on $(^3\mathrm{He},t)$ reaction at Saturne [8,9]. In these experiments, the energy/momentum distributions of ejectile, i.e., n in (p,n) and t in $(^3\mathrm{He},t)$ reactions, were measured at the forward angle in coincidence with either a pair of π^+ and p or two or three protons or single π^+ emitted within the 4π directions. In the experiment done at KEK, proton beam of 1.5 GeV/c momentum had been made to collide with proton and ^{12}C targets. Various charged particles emitted in coincidence with the forward going neutron were detected in a large acceptance (covering 88% of the total solid angle) spectrometer called FANCY. Similar results also had been found in the exclusive measurement done at Saturne on $^{12}\mathrm{C}(^3\mathrm{He},t)$ reaction at 2 GeV beam energy. Various charged particles emitted in coincidence with the forward going triton were detected within the 4π detector called DIOGENE. Additionally, in this experiment the angular correlation between the momentum transfer to target and the momentum of pion emitted in the final state had been established [9]. The results from these exclusive measurements deploy one to one correspondence with those obtained from the pion nuclear scatterings, i.e.,

pion-proton in coincidence ↔ pion quasielastic scattering,

proton-proton in coincidence ↔ two-body pion absorption,

coherent pion production ↔ pion elastic scattering.

The spectra measured in the exclusive experiments show that both *pp* event and coherent π^+ production are the key ingredients for the shift of Δ peak seen in the inclusive measurements. Among themselves, the coherent π^+ production

channel contributes dominantly to the inclusive spectra. These two channels do not exist for the proton target. In contrast, the $\pi^+ p$ event for nuclear targets shows an insignificant shift with respect to that for the hydrogen target [8,10].

Analyses of the data obtained from the above exclusive measurements envisage that the various exit channels seen in these experiments arise due to various dampening processes for $\Delta(1232)$ occurring in the nucleus. The in-coincident $\pi^+ p$ event arises due to the quasifree decay of Δ^{++} produced on the nuclear surface. Therefore, the spectrum for the $\pi^+ p$ emission from nuclei does not show any significant difference from that obtained for the hydrogen target. The in-coincident *pp* event arises due to the Δ conversion process, such as $\Delta N \rightarrow pp$, taking place in the nuclear medium. Thus, the *pp* event originates from the deeper inside of the nucleus, and hence must be forbidden for the hydrogen target. Microscopic calculations on the reaction mechanisms for these Δ dampening processes have been presented in Refs. [11,12].

Coherent π^+ production process can be thought as a kind of elastic scattering, where the virtual pion emitting from the projectile propagates through the nucleus by mixing with the Δ-hole states and ends up as an on-shell pion. This conversion process is possible since the recoil nucleus, as a whole, can adjust the momentum needed to put this off-shell pion on its mass shell. The peak for the measured coherent π^+ distribution [7,9] shows a considerable downward energy shift revealing an information complementary to that of real pion scattering on the nucleus. The measured angular distribution for the coherent π^+ emission [9] shows that it is strongly forward (in the direction of momentum transfer) peaked. This observation exhibits an intimate relationship with the elastic pion nuclear scattering [13]. Theoretical investigations [14] reveal that both effects, i.e., the downward energy shift and the peaking in forward direction, seen in the coherent π^+ production spectrum occur due to the longitudinal part of the $NN \rightarrow N\Delta$ interaction. The importance of the coherent π^+ emission channel, in context to the peak position observed in the inclusive measurements, is also analyzed by several authors [15,16]. According to their studies, the contribution of this channel in addition to those due to various other channels is absolutely necessary to reproduce the Δ-peak position seen in the inclusive measurements.

Encouraged by the observed qualitative similarity between the spectra in the inclusive/exclusive measurements and in the real pion induced reactions, as described before, in the present work it has been explored that the extent up to which the measured inclusive spectra and the coherent π^+ production data can be accounted for by the real pion scattering on the nucleus. Since the data for the forward going ejectile energy/momentum distributions are available for the $^{12}C(^3He,t)$ and $^{12}C(p,n)$ reactions, the corresponding calculations have been presented here. The peripheral nature of these reactions is incorporated through the use of distorted waves for the projectile and ejectile. The calculated results reproduce the measured distributions reasonably well.

However, it should be mentioned that in the $\Delta(1232)$-excitation region the contribution from one pion exchange interaction alone is sufficient to reproduce the measured spin averaged cross section. For example, the detailed experimental studies by Wicklund *et al.* [17] demonstrate that the pion exchange interaction gives a very good fit to the data for the spin averaged $pp \rightarrow n\Delta^{++}$ reaction over a wide kinematic region. This finding also, for beam energies from threshold to very high, has been corroborated by Dmitriev *et al.* [18] and Jain *et al.* [19]. They also show that any inclusion of rho exchange interaction yields very unsatisfactory results. In the relatively recent work due to Kundu *et al.* [20], they have shown that the $\Delta(1232)$ excitation due to one pion exchange interaction only is in very well accord with the measured spin averaged cross sections for the elementary $p(p,p'\pi^+)n$ reaction. In another study, Jain and Santra [21] find that while the rho exchange interaction is absolutely essential to account for the $p(n,p)n$ data, it is not at all favored by the $p(p,n)\Delta^{++}$ data. The reason for this disfavor of the rho exchange interaction in this delta excitation, to a certain extent, is provided by a microscopic study for the $\rho N\Delta$ vertex by Haider *et al.* [22], where they find that the microscopically calculated value of the $\rho N\Delta$ coupling constant is much smaller than the normally assumed value.

Only one pion exchange interaction also has been found to give satisfactory results on $\Delta(1232)$ excitation in nuclei, when the beam is unpolarized. Using one pion exchange interaction only, Dmitriev [16] has successfully reproduced the data of the spin averaged cross sections for the inclusive $(^3He,t)$ reaction on ^{12}C nucleus in this Δ excitation region. Beside this, our earlier works [11,23], considering the $\Delta(1232)$ excitation due to one pion exchange interaction only, have accounted very well for the spin averaged cross sections measured for various Δ^{++}-decay channels, i.e., $\pi^+ p$ and *pp* events, in the exclusive (p,n) [7] and $(^3He,t)$ [8] reactions. Recent analysis due to Kundu and Jain [24] on the measured spin averaged cross sections for the $^6Li(p,\Delta^{++})^6He$ reaction [25] shows that the use of one pion exchange interaction only for the $\Delta(1232)$ excitation fits the data for this reaction absolutely.

With polarized beams, however, considerable strength has been found to lie in the transverse mode [26]. In one pion exchange model, this strength, as Dmitriev [27] and Sams *et al.* [28] have shown, can arise, to a large extent, from the beam distortion. Therefore, the role of rho exchange interaction in the $\Delta(1232)$ excitation at best can be thought to be controversial. As mentioned above, it is not required to reproduce the spin averaged cross sections in this Δ excitation region [29], only the data from the spin transfer measurements show some indication for it. The present work deals only with the spin averaged cross section in the $\Delta(1232)$-excitation region. Therefore, in this work the contribution from the one pion exchange interaction only has been incorporated, which is very much consistent with other investigations made by several authors in this field.

In Sec. II, the formalism is given for the Δ and coherent pion production in the charge exchange reaction. In Sec. III, the calculated cross sections have been compared with the measured distributions.

II. FORMALISM

In the charge exchange reactions considered here, the projectile emits π^+, and subsequently it becomes the ejectile. In the process of this transition, the spin-isospin configuration of the projectile gets changed, while the space coordinates are assumed to remain unchanged. The pion, emitting from the projectile, interacts with the target nucleus leading to various channels in the final state. Therefore, the virtual pion source can be described by the πNN Lagrangian $\mathcal{L}_{\pi NN}$. It, in pseudovector presentation, can be written as

$$\mathcal{L}_{\pi NN}=\frac{fF(q^2)}{m_\pi}\bar{N}\gamma^\nu\gamma^5\boldsymbol{\tau}N\cdot\partial_\nu\boldsymbol{\pi}, \tag{1}$$

where f and $F(q^2)$ are the coupling constant and the form factor at the πNN vertex. The value of f is taken equal to 1.008. In the monopole form, $F(q^2)$ is given by

$$F(q^2)=\frac{\Lambda^2-m_\pi^2}{\Lambda^2-q^2}, \tag{2}$$

with $q^2=w^2-\mathbf{q}^2$. Here, w and $\mathbf{q}$ are the energy and the momentum respectively carried by the virtual pion. Λ appearing in this equation is taken equal to 1200 MeV/c.

The standard reaction model leads to an ansatz [30] that the cross section of a nuclear scattering can be approximated by the corresponding plane wave cross section multiplied by an attenuation factor to account for the absorption of the continuum particles. This attenuation factor, in fact, estimates the probability for a nuclear particle seen by the probes. For the eikonally distorted waves of projectile and ejectile, the expression for the attenuation factor $\mathcal{A}$ is

$$\mathcal{A}=\frac{\int d\mathbf{b}e^{-2Im\,\delta(\mathbf{b})}T(\mathbf{b})}{\int d\mathbf{b}T(\mathbf{b})}, \tag{3}$$

where $\delta(\mathbf{b})$ is the sum of the phase shifts for projectile and ejectile at the impact parameter $\mathbf{b}$. $T(\mathbf{b})$ is the nuclear thickness function, which, in terms of nuclear density $\varrho(\mathbf{r})$, is given by

$$T(\mathbf{b})=\int_{-\infty}^{+\infty}dz\,\varrho(\mathbf{r});\quad \mathbf{r}=\mathbf{b}+\hat{z}z. \tag{4}$$

The differential cross section for the inclusive (a,b) reaction on a spin-zero target nucleus can be written as

$$d\sigma=\mathcal{A}\frac{2\pi}{v_a}\frac{m_am_b}{E_aE_b}\sum_n\delta(w-w_n)\times\frac{1}{(2s_a+1)}\sum_{m_{s_a}m_{s_b}}|T_{n0}|^2\frac{d\mathbf{k}_b}{(2\pi)^3}. \tag{5}$$

In this equation, "n" denotes the state of the nucleus after the scattering takes place, whereas "0" represents the ground state of the target nucleus. E_a and E_b are the energies of the projectile a and the ejectile b, respectively, and $w(=E_a-E_b)$ is the energy transfer to the nucleus.

The T matrix, T_{n0} appearing in the above equation, in PWBA is given by

$$T_{n0}=\langle k_b,(n,b|\hat{V}|a,0),k_a\rangle, \tag{6}$$

where $\hat{V}$ describes the interacting potential. For one pion exchange interaction, $\hat{V}$ can be presented as

$$\hat{V}=\hat{\Gamma}_{\pi NN}G_\pi(q^2)\hat{\Gamma}_{\pi A}. \tag{7}$$

Here, $\hat{\Gamma}_{\pi NN}$ represents the pion mediated NN interaction operator at the projectile-ejectile vertex, which could be described by $\mathcal{L}_{\pi NN}$ in Eq. (1) except the field functions appearing in it. $\hat{\Gamma}_{\pi A}$ is the operator describing the interaction of virtual pion with the nucleus. $G_\pi(t)$ describes the propagation of the virtual pion, which, in the relativistic presentation, has the form

$$G_\pi(q^2)=-\frac{1}{m_\pi^2-q^2}, \tag{8}$$

with $m_\pi(=140\ \text{MeV})$ being the mass of pion.

Using the potential $\hat{V}$ appearing in Eq. (7), the double differential cross section in Eq. (5) for the ejectile energy distribution can be factorized as

$$\frac{d^2\sigma}{dE_bd\Omega_b}=\mathcal{A}\frac{m_am_bk_b}{(2\pi)^2k_a}\langle|\Gamma_{\pi ab}(q^2)|^2\rangle|G_\pi(q^2)|^2S(w,\mathbf{q}). \tag{9}$$

Where the factor $\langle|\Gamma_{\pi ab}(q^2)|^2\rangle$ in this equation denotes the πab vertex factor. It acts as a source function for the virtual pion, and is defined as

$$\langle|\Gamma_{\pi ab}(q^2)|^2\rangle\equiv\frac{1}{2s_a+1}\sum_{m_{s_a},m_{s_b}}|\langle k_b,b|\hat{\Gamma}_{\pi NN}|a,k_a\rangle|^2. \tag{10}$$

Forms of $\langle|\Gamma_{\pi ab}(q^2)|^2\rangle$ for (p,n) and $(^3\text{He},t)$ reactions will be presented in the subsequent subsections.

$S(w,\mathbf{q})$ in Eq. (9) is commonly known as the dynamical structure factor. It, as given in Ref. [31], is defined as

$$S(w,\mathbf{q})\equiv\sum_n\delta(w-w_n)|\langle n|e^{i\mathbf{q}\cdot\mathbf{r}}\hat{\Gamma}_{\pi A}|0\rangle|^2. \tag{11}$$

In nuclear matter $S(w,\mathbf{q})$, as subtled in the above reference, can be associated with the imaginary part of the pion self-energy $Im\Pi(w,\mathbf{q})[=2wW(w,\mathbf{q})$, where $W(w,\mathbf{q})$ is the imaginary part of the pion optical potential] as

$$S(w,\mathbf{q})=-\frac{2w}{\pi}W(w,\mathbf{q}). \tag{12}$$

Furthermore, the imaginary part of the optical potential attenuates the flux of the particles, i.e., it removes the flux

from the incident and the elastically scattered waves. Therefore, this potential is related to the total reaction cross section, which incorporates both inelastic and absorptive processes [32]. Hence, $W(w,\mathbf{q})$ can be expressed as

$$W(w,\mathbf{q}) = -\frac{|\mathbf{q}|}{2w}\sigma_r(w), \tag{13}$$

where $\sigma_r(w)$ denotes the total reaction cross section for the virtual pion. With this expression of $W(w,\mathbf{q})$, the dynamical structure factor $S(w,\mathbf{q})$ in Eq. (12), is given by

$$S(w,\mathbf{q}) = \frac{|\mathbf{q}|}{\pi}\sigma_r(w). \tag{14}$$

Using the above expression for $S(w,\mathbf{q})$, the cross section given in Eq. (9) can be written as

$$\left(\frac{d^2\sigma}{dE_b d\Omega_b}\right)_r = \mathcal{A}\frac{m_a m_b k_b}{(2\pi)^2 k_a}\langle|\Gamma_{\pi ab}(q^2)|^2\rangle|G_\pi(q^2)|^2\frac{|\mathbf{q}|}{\pi}\sigma_r(w). \tag{15}$$

This equation describes all inelastic and absorptive processes induced by the virtual pion beam of four momenta determined by the kinematics of projectile and ejectile. To indicate these reactive processes, the subscript "r" has been introduced to the left hand side of this equation. This expression has been successfully used to analyze the measured multiproton emission spectra for both ^{12}C(p,n) and ^{12}C$(^3$He$,t)$ reactions [23]. Writing $\sigma_r(w)$ in terms of total and elastic scattering cross sections, i.e., $\sigma_r(w) = \sigma_t(w) - \sigma_{el}(w)$, the above equation can be split into two parts. One part would involve the total scattering cross section $\sigma_t(w)$, while the other part would contain the total elastic scattering cross section $\sigma_{el}(w)$. These two parts can be presumably written as

$$\left(\frac{d^2\sigma}{dE_b d\Omega_b}\right)_{inc} = \mathcal{A}\frac{m_a m_b k_b}{(2\pi)^2 k_a}\langle|\Gamma_{\pi ab}(q^2)|^2\rangle|G_\pi(q^2)|^2\frac{|\mathbf{q}|}{\pi}\sigma_t(w), \tag{16}$$

and

$$\left(\frac{d^2\sigma}{dE_b d\Omega_b}\right)_{coh} = \mathcal{A}\frac{m_a m_b k_b}{(2\pi)^2 k_a}\langle|\Gamma_{\pi ab}(q^2)|^2\rangle|G_\pi(q^2)|^2\frac{|\mathbf{q}|}{\pi}\sigma_{el}(w). \tag{17}$$

In principle, $\sigma_t(w)$ includes the contributions from all channels in the virtual pion induced reaction. Therefore, the expression in Eq. (16) containing $\sigma_t(w)$ would pertain to be the double differential cross section for the inclusive (a,b) reaction. The expression in Eq. (17), which contains $\sigma_{el}(w)$, can be thought of as describing the elastic scattering of virtual pion and hence, this would represent the coherent pion emission in (a,b) reaction.

III. RESULTS AND DISCUSSION

In inclusive measurements, as described earlier, the energy/momentum distribution for ejectile is used to measure without detecting any other particles emitting from the target nucleus. The data for the zero degree inclusive (p,n) reaction on ^{12}C nucleus at various energies are available from LAMPF [3], whereas the same for the $(^3$He$,t)$ reaction exist from Saturne [5]. To analyze these data, the double differential cross sections for the energy/momentum distribution of the forward going ejectile, i.e., n in (p,n) and t in $(^3$He$,t)$ reactions, have been calculated here. Along with these, calculations also are presented to account the data for the coherent π^+ production. For this exclusive channel, the data are available for the ^{12}C(p,n) reaction at 1.5 GeV/c beam momentum from KEK [7], and also from Saturne for the^{12}C$(^3$He$,t)$ reaction at 2 GeV beam energy [9]. In these exclusive measurements, the energy/momentum distributions for the ejectile were measured in coincidence with π^+ detected in a large acceptance [(85–88)% of 4π] detector placed around the target. Due to angle and energy cuts in the detecting systems for these measurements, the magnitudes of cross sections could not have been determined absolutely. Rather, as mentioned before, these measurements show that the coherent π^+ scattering on nucleus is closely associated with the elastic pion nuclear scattering.

For the calculations to reproduce the data from the inclusive measurements on ^{12}C(p,n) and ^{12}C$(^3$He$,t)$ reactions, the total virtual π^+ scattering cross section, i.e., $\sigma_t(w)$ in Eq. (16), on ^{12}C nucleus is required as an input quantity for its energy range of about 150–500 MeV. Whereas, in this energy range calculations to account the data for coherent π^+ production in the exclusive experiments on ^{12}C(p,n) and ^{12}C$(^3$He$,t)$ reactions need the total elastic virtual π^+ scattering cross section, i.e., $\sigma_{el}(w)$ in Eq. (17), on^{12}C nucleus. As it is exhibited in our earlier work [23], for the energy region considered here, the energy-momentum dispersion curves for the real and virtual pion look very much similar. Besides, for a fixed pion energy, the momentum for the virtual pion, compared to that for the real pion, is larger. Due to this qualitative similarity, as presented in Ref. [23], the replacement of the virtual pion nuclear absorption cross sections by the corresponding measured values for the real pion of same energy works very well to reproduce the measured shape for the multiproton emission in the charge exchange reactions [7,8] in the $\Delta(1232)$-excitation region. Complementary to this, the virtual pion induced total and elastic scattering cross sections, as required for the present calculations, have been approximated by the corresponding measured values for the real pion. For the required energy range of pion, the measured total cross sections for the π^+ scattering on ^{12}C nucleus are reported in Ref. [33], and the total elastic π^+ scattering cross sections for the same nucleus are due to Ashery *et al.* [34]. These cross sections, in the present work, are used as the inputs to calculate the ejec-

tile energy/momentum distribution spectra for these inclusive and exclusive reactions.

The attenuation factor $\mathcal{A}$ due to the absorption for the continuum particles, as shown in Eq. (3), has to be estimated through the imaginary part of the phase shifts, $Im\,\delta(\mathbf{b})$, for projectile and ejectile, and the thickness function, $T(\mathbf{b})$ as defined in Eq. (4), for the nucleus. For ^{12}C nucleus, the density distribution $\varrho(\mathbf{r})$ required to evaluate $T(\mathbf{b})$ is given by

$$\varrho(\mathbf{r}) = \varrho(0)[1 + a(r/c)^2]e^{-(r/c)^2}, \tag{18}$$

where the values of a and c are taken equal to 1.247 and 1.649 fm, respectively [35].

The expressions for $Im\,\delta(\mathbf{b})$, appearing in Eq. (3), and vertex factors, $\langle|\Gamma_{\pi ab}(q^2)|^2\rangle$ in Eqs. (16) and (17), for (p,n) and (^{3}He,t) reactions will be presented in the following sections.

A. ^{12}C(p,n) reaction

For the inclusive and exclusive (p,n) reactions presented here, the virtual pion source function $\langle|\Gamma_{\pi ab}(q^2)|^2\rangle$ appearing in Eqs. (16) and (17) would be the $\pi^+ pn$ vertex factor $\langle|\Gamma_{\pi^+ pn}(q^2)|^2\rangle$. The expression for it is given by

$$\langle|\Gamma_{\pi^+ pn}(q^2)|^2\rangle = -2\left|\frac{fF(q^2)}{m_\pi}\right|^2 q^2, \tag{19}$$

with $q^2 = (E_p - E_n)^2 - (\mathbf{k}_p - \mathbf{k}_n)^2$.

The phase shift $\delta(\mathbf{b})$, required to calculate the attenuation factor $\mathcal{A}$ in Eq. (3), is composed of the phase shifts for proton and neutron, i.e., $\delta(\mathbf{b}) = \delta_p(\mathbf{b}) + \delta_n(\mathbf{b})$. The imaginary part of it for a nucleon scattered by a nucleus can be written as

$$Im\,\delta_N(\mathbf{b}) = -\frac{1}{v_N}\int_0^\infty Im V_{ON}(\mathbf{b},z)\,dz, \tag{20}$$

with N being a proton or a neutron. v_N and $V_{ON}(\mathbf{b},z)$ represent the velocity and the optical potential for the nucleon. Using the high energy ansatz, the imaginary part of $V_{ON}(\mathbf{b},z)$ is given by

$$Im V_{ON}(\mathbf{b},z) = -\frac{k_{NN}}{2E_{NN}}\sigma_t^{NN}\varrho(\mathbf{r}); \quad \mathbf{r} = \mathbf{b} + \hat{z}z, \tag{21}$$

where k_{NN} denotes the momentum in the nucleon-nucleon center-of-mass system. σ_t^{NN} is the total nucleon-nucleon scattering cross section. $\varrho(\mathbf{r})$ represents the spatial distribution of $V_{ON}(\mathbf{b},z)$. Here, this distribution is assumed to be identical to that for the nuclear density and hence, it can be described by Eq. (18) for ^{12}C nucleus.

For the inclusive ^{12}C(p,n) reaction, the double differential cross sections $(d^2\sigma)/(dk_n d\Omega_n)$, for the forward going neutron momentum k_n distribution, have been calculated here. These results are compared with the available data [3] in Fig. 1 for the beam energies equal to 647 MeV and 800 MeV. This figure shows that for both of these energies the calculated results, after dividing by a factor of about 2.5, reproduce the data around the Δ peak very well. However,

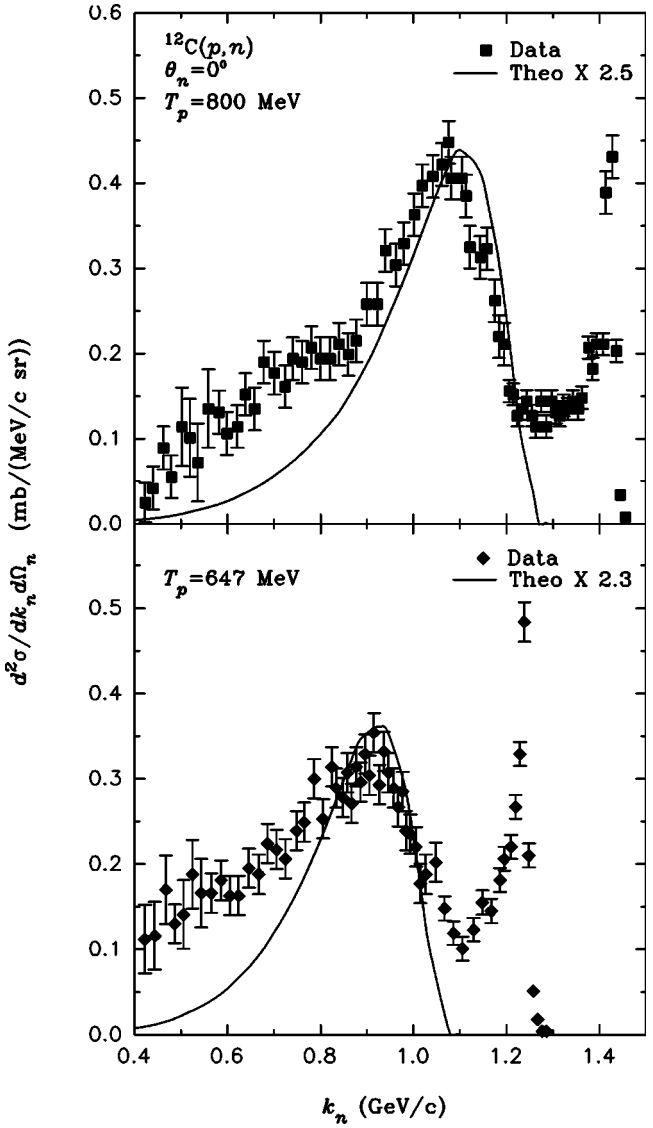

FIG. 1. Calculated double differential cross sections for the forward going neutron momentum distribution at the beam energies equal to 647 MeV and 800 MeV. Data are taken from Ref. [3]. The calculated curves are normalized to the peak of the measured spectra.

even after this scaling, the present calculation underestimates the cross sections in the region below Δ peak. This discrepancy can be accounted for due to the unavoidable drawback of the (p,n) reaction as a probe to investigate the Δ excitation in nucleus. The neutron arising due to the decay of Δ isobar was also detected in this measurements. This neutron, in an obvious reason, would have lower energies than that produced by Δ isobar, but it can have partial overlap with the main quasifree Δ peak. In contrast, this decay background, as shown latter, is not seen in the (^{3}He,t) reactions on nucleus. This is due to the small probability for the excited projectile, i.e., ^{3}He, decaying to triton, and also the latter from the quasifree decay of the target nucleus are expected to be very less (see in Refs. [36,37]).

In Fig. 2, the calculated results for the coherent π^+ emission in ^{12}C(p,n) reaction have been presented along with the

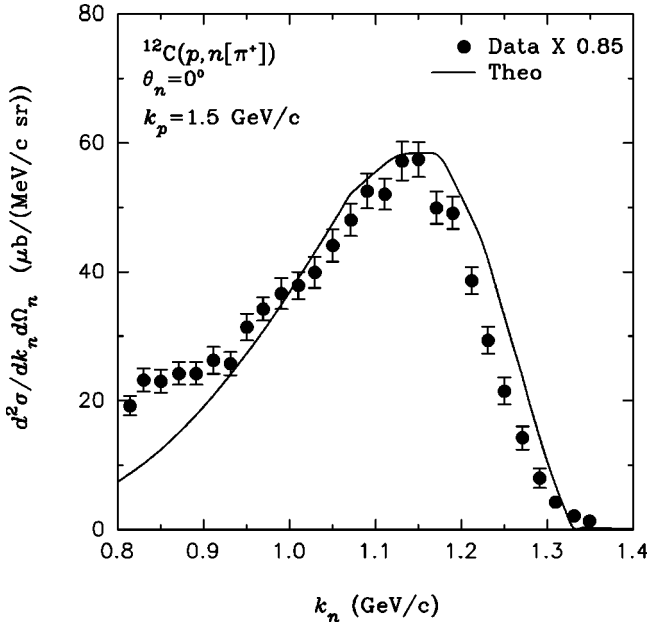

FIG. 2. Calculated neutron momentum distribution spectrum for the coherent π^+ emission within 4π directions. Data are taken from Ref. [7], and scaled to the calculated peak cross section (see text).

corresponding measured spectrum from KEK [7] at the beam momentum equal to 1.5 GeV/*c*. Since the magnitudes of the measured cross sections are not available with certainty, they have been given relative to the calculated peak cross section. This figure shows that the shape of the calculated spectrum agrees very well with the measured distribution almost in the whole range of neutron momentum. Here also, the enhancement seen in the measured cross sections below the neutron momentum equal to 900 MeV/*c*, as discussed before, could be due to the background effect.

B. ^{12}C(^{3}He,*t*) reaction

The vertex factor $\langle|\Gamma_{\pi ab}(q^2)|^2\rangle$ in Eqs. (16) and (17) for the (^{3}He,*t*) reaction would be the $\pi^+{}^3$He*t* vertex factor $\langle|\Gamma_{\pi^+ht}(q^2)|^2\rangle$. The notation "*h*" in the subscript has been used in place of ^{3}He, and the same will be followed for other terms also. This vertex factor differs in a major way from that of (p,n) reaction by the form factor for the helium-3 to triton transition. $\langle|\Gamma_{\pi^+ht}(q^2)|^2\rangle$ is given by

$$\langle|\Gamma_{\pi^+ht}(q^2)|^2\rangle = -2\left|\frac{fF(q^2)}{m_\pi}\tilde{\varrho}_{h\to t}(q^2)\right|^2 q^2, \qquad (22)$$

with q^2 being the four-momentum transfer from the ^{3}He and *t* vertex to nucleus. In this equation, $\tilde{\varrho}_{h\to t}(q^2)$ denotes the helium-3 to triton transition density. This transition density, as constructed by Dmitriev *et al.* [18], is

$$\tilde{\varrho}_{h\to t}(q^2) = \exp(a_1 q^2)[1 + b_1 q^4], \qquad (23)$$

with $a_1 = 11.15$ GeV^{-2} and $b_1 = 14$ GeV^{-4}. This form fits the electron scattering data for the form factors of mass-3 particles up to the momentum transfer $\leqslant 8$ fm^{-2}.

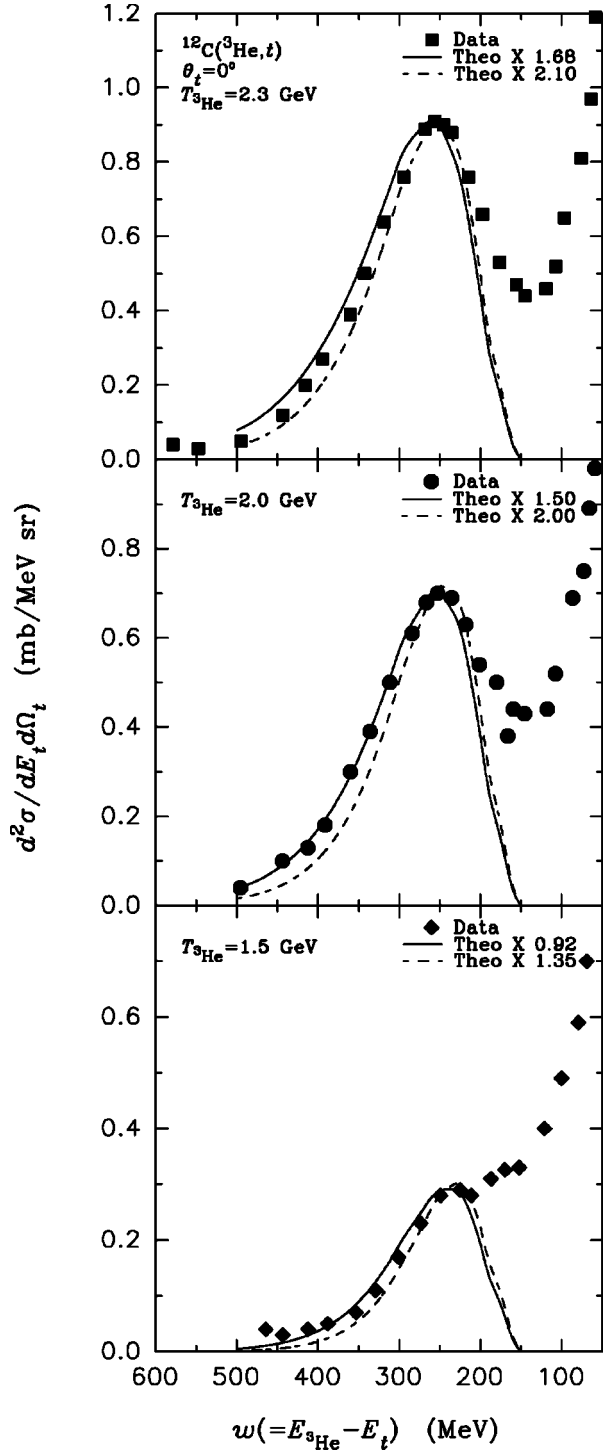

FIG. 3. Calculated missing energy distribution spectra for the forward going triton at various beam energies. Data are taken from Ref. [5]. Solid and dashed curves represent the calculated cross sections for the helium-3 to triton transition densities given in Eqs. (23) and (24), respectively. The calculated curves are normalized to the peak of the measured spectra.

Also, $\tilde{\varrho}_{h\to t}(q^2)$ can be approximated by the following magnetic form factor of ^{3}He:

$$\tilde{\varrho}_{h\to t}(q^2) = \exp(a_2^2 q^2) + b_2^2 q^2 \exp(c_2^2 q^2), \qquad (24)$$

with $a_2=0.654$ fm, $b_2=0.456$ fm, and $c_2=0.821$ fm. This form has been extracted up to the momentum transfer equal to 16 fm^{-2} by McCarthy *et al.* [38] from the electron scattering data between 170 and 750 MeV on ^{3}He.

To estimate the attenuation factor, $\mathcal{A}$ in Eq. (3), for the (^{3}He,t) reaction, the phase shift $\delta(\mathbf{b})$ also, in principle, can be constructed from the optical potential. Since the latter for a mass-3 particle is poorly known, the measured phase shift has been preferred in the present work. In fact, the information about the measured phase shift in between 1 and 2 GeV, as required for this calculation, exists only for the α-elastic scattering at 1.37 GeV on calcium isotopes [39]. For this reaction, $\exp[i\delta(b)]$, which describes the data very well, is purely absorptive and has the following form:

$$e^{-Im\,\delta(b)}=\frac{1}{1+e^{-(b-R)/d}}, \tag{25}$$

with $R=r_0A^{1/3}$ fm. Here, A denotes the mass number of the nucleus. The values of the radius parameter r_0 and the diffuseness d are found equal to 1.45 fm and 0.68 fm, respectively. Since the mass-3 particles are known to have lesser absorption than alpha particle, and due to lack of availability of any other information, the above form has been taken for the present purpose of describing the attenuation of ^{3}He and t except the value of r_0 is reduced to 1.2 fm [40].

For the inclusive ^{12}C(^{3}He,t)reaction, the double differential cross sections $(d^2\sigma)/(dE_t d\Omega_t)$, for the missing energy $w(=E_{^3\mathrm{He}}-E_t)$ distribution of the forward going triton, have been calculated to reproduce the data obtained from the corresponding measurements. The calculated distributions are compared with the measured spectra in Fig. 3 for the beam energies equal to 1.5, 2.0, and 2.3 GeV. The experimental points have been taken from the Ref. [5]. In this figure, the solid curve represents the calculated cross sections for the helium-3 to triton transition density, $\tilde{\varrho}_{h\to t}(q^2)$, given in Eq. (23), while the dashed curve is due to $\tilde{\varrho}_{h\to t}(q^2)$ taken from Eq. (24). The calculated curves are normalized to the peak of the measured spectra. Here, the agreement between calculated and measured energy spectra is quite satisfactory, however, the calculated peak cross section comes within a factor of about 2.

In Fig. 4, the calculated coherent π^+ production spectra in the (^{3}He,t) reaction have been presented along with the data. The experimental points are taken from the measurement done at Saturne [9] for the beam energy equal to 2 GeV. Here also, the solid and the dashed curves represent the calculated cross sections due to two different forms of

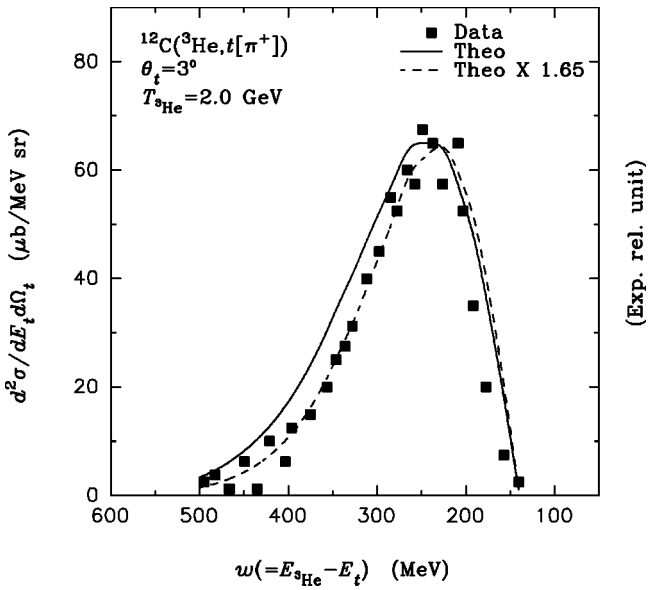

FIG. 4. Calculated triton missing energy distribution spectra for the coherent π^+ emission within 4π directions. Data are taken from Ref. [9]. Solid and dashed curves represent the calculated cross sections for the helium-3 to triton transition densities given in Eqs. (23) and (24), respectively. The measured spectrum and the dashed curve are scaled to the peak of the solid curve (see text).

$\tilde{\varrho}_{h\to t}(q^2)$ as given in Eqs. (23) and (24), respectively. Since the absolute magnitudes of the data are not available, the measured spectrum and the dashed curve have been scaled to the peak of the solid curve. The calculated results, as shown in this figure, reproduce the measured spectrum very well.

IV. CONCLUSIONS

From the investigations presented here, it can be concluded that the distinct $\Delta(1232)$ excitation in nucleus, as seen in the inclusive (p,n) and (^{3}He,t) reactions, can be described successfully by the real pion induced reactions on the nucleus. Also, the coherent π^+ emission in the charge exchange reactions can be accounted for satisfactorily by the elastic scattering of real pion on the nucleus.

ACKNOWLEDGMENTS

I gratefully thank Dr. S. Kailas, Head of the Nuclear Physics Division, for his support and encouragement to carry out this work. I also thank Narayan Rao and V. T. Nimje for their suggestions during the preparation of this manuscript.

[1] T. Ericson and W. Weise, *Pions and Nuclei* (Clarendon, Oxford, 1988); T.E.O. Ericson, in *The Building Blocks of Nuclear Structure, Amalfi, Italy, 1992*, edited by Aldo Covello (World Scientific, Singapore, 1992), p. 3.

[2] B.E. Bonner *et al.*, Phys. Rev. C **18**, 1418 (1978); C.W. Bjork *et al.*, Phys. Lett. **63B**, 31 (1976); G. Glass *et al.*, Phys. Rev. D **15**, 36 (1977); D.A. Lind, Can. J. Phys. **65**, 637 (1987).

[3] C.G. Cassapakis *et al.*, Phys. Lett. **63B**, 35 (1976).

[4] C. Ellegaard *et al.*, Phys. Lett. **154B**, 110 (1985); Phys. Rev. Lett. **50**, 1745 (1983); Can. J. Phys. **65**, 600 (1987); I. Bergqvist *et al.*, Nucl. Phys. **A469**, 648 (1987); V.G. Ableev *et al.*, JETP Lett. **40**, 763 (1984); D. Bachelier *et al.*, Phys.

Lett. B **172**, 23 (1986); M. Roy-stephan, Nucl. Phys. **A488**, 187c (1988); C. Gaarde, Annu. Rev. Nucl. Part. Sci. **41**, 187 (1991).
[5] D. Contardo *et al.*, Phys. Lett. **B168**, 331 (1986).
[6] H. Esbensen and T.-S.H. Lee, Phys. Rev. C **32**, 1966 (1985); E. Oset, E. Shino, and H. Toki, Phys. Lett. B **224**, 249 (1989); V.F. Dmitriev, *ibid.* **226**, 219 (1989); T. Udagawa, S.-W. Hong, and F. Osterfeld, *ibid.* **245**, 1 (1990); J. Delorme and P.A.M. Guichon, *ibid.* **263**, 157 (1991).
[7] J. Chiba *et al.*, Phys. Rev. Lett. **67**, 1982 (1991).
[8] T. Hennino *et al.*, Phys. Lett. B **283**, 42 (1992).
[9] T. Hennino *et al.*, Phys. Lett. B **303**, 236 (1993).
[10] P. Radvanyi *et al.*, in *Hadrons in Nuclear Matter*, edited by H. Feldmeier and W. Nörenberg (GSI, Darmstadt, 1995), p. 44.
[11] B.K. Jain and Swapan Das, Phys. Rev. C **50**, 370 (1994); B.K. Jain, Swapan Das, and A.B. Santra, in *Proceedings of RIKEN International Workshop on Delta Excitation in Nuclei, 1993, Wako shi, Japan*, edited by H. Toki, M. Ichimura, and M. Ishihara (World Scientific, Singapore, 1994), p. 123.
[12] B. Körfgen, P. Oltmanns, F. Osterfeld, and T. Udagawa, Phys. Rev. C **55**, 1819 (1997).
[13] B. Körfgen, F. Osterfeld, and T. Udagawa, Phys. Rev. C **50**, 1637 (1994).
[14] P.F. de Córdoba, E. Oset, and M.J. Vicente-Vacas, Nucl. Phys. **A592**, 472 (1995); P. Oltmanns, F. Osterfeld, and T. Udagawa, Phys. Lett. B **299**, 194 (1993); F. Osterfeld, B. Körfgen, P. Oltmanns, and T. Udagawa, Phys. Scr. **48**, 95 (1993).
[15] P.F. de Córdoba, J. Nieves, E. Oset, and M.J. Vicente-Vacas, Phys. Lett. B **319**, 416 (1993); E. Oset, P.F. de Córdoba, J. Nieves, and M.J. Vicente-Vacas, Phys. Scr. **48**, 101 (1993).
[16] V.F. Dmitriev, Phys. Rev. C **48**, 357 (1993).
[17] A.B. Wicklund *et al.*, Phys. Rev. D **34**, 19 (1986); **35**, 2670 (1987).
[18] V. Dmitriev, O. Sushkov, and C. Gaarde, Nucl. Phys. **A459**, 503 (1986).
[19] B.K. Jain and A.B. Santra, Nucl. Phys. **A519**, 697 (1990); Phys. Lett. B **244**, 5 (1990).
[20] Bijoy Kundu, B.K. Jain, and A.B. Santra, Phys. Rev. C **58**, 1614 (1998); **61**, 049902(E) (2000).
[21] B.K. Jain and A.B. Santra, Phys. Rev. C **46**, 1183 (1992).
[22] Q. Haider and L.C. Liu, Phys. Lett. B **335**, 253 (1994).
[23] B.K. Jain and Swapan Das, Phys. Lett. B **386**, 33 (1996).
[24] Bijoy Kundu and B.K. Jain, Phys. Lett. B **422**, 19 (1998).
[25] T. Hennino *et al.*, Phys. Rev. Lett. **48**, 997 (1982).
[26] D. Prout *et al.*, Nucl. Phys. **A577**, 233c (1994); Phys. Rev. Lett. **76**, 4488 (1996); C. Ellegaard *et al.*, Phys. Lett. B **231**, 365 (1989).
[27] V. Dmitriev, Nucl. Phys. **A577**, 249c (1994).
[28] T. Sams and V.F. Dmitriev, Phys. Rev. C **45**, R2555 (1992).
[29] V.F. Dmitriev (private communication).
[30] R.D. Smith, in *Spin Observables of Nuclear Probes*, edited by C.J. Horowitz, C.D. Goodman, and G.E. Walker (Plenum, New York, 1988), p. 15.
[31] A.L. Fetter and J.D. Walecka, *Quantum Theory of Many Particles* (McGraw-Hill, New York, 1971).
[32] L.I. Schiff, *Quantum Mechanics* (McGraw-Hill, New York, 1968), p. 131.
[33] A.S. Clough *et al.*, Nucl. Phys. **B76**, 15 (1974); A.S. Carroll *et al.*, Phys. Rev. C **14**, 635 (1976).
[34] D. Ashery *et al.*, Phys. Rev. C **23**, 2173 (1981).
[35] H.De. Vries and C.W. De Jager, At. Data Nucl. Data Tables **36**, 495 (1987).
[36] R.G. Jeppesen, Ph.D thesis, University of Colorado, 1986.
[37] T. Udagawa, P. Oltmanns, F. Osterfeld, and S.W. Hong, Phys. Rev. C **49**, 3162 (1994).
[38] J.S. McCarthy, I. Sick, and R.R. Whitney, Phys. Rev. C **15**, 1396 (1977).
[39] D.C. Choudhury, Phys. Rev. C **22**, 1848 (1980).
[40] B.K. Jain, Phys. Rev. C **32**, 1253 (1985); N.G. Kelkar and B.K. Jain, Int. J. Mod. Phys. E **4**, 181 (1995).